

Received October 3, 2017, accepted November 8, 2017, date of publication November 28, 2017, date of current version February 14, 2018.

Digital Object Identifier 10.1109/ACCESS.2017.2778184

An Electrically Actuated DC-to-11-GHz Liquid-Metal Switch

MATTHEW R. MOOREFIELD¹, (Student Member, IEEE), RYAN C. GOUGH¹, (Member, IEEE), AARON T. OHTA¹, (Senior Member, IEEE), AND WAYNE A. SHIROMA¹, (Senior Member, IEEE)

Department of Electrical Engineering, University of Hawai'i at Mānoa, Honolulu, HI 96822 USA

Corresponding author: Wayne A. Shiroma (shiroma@ieee.org)

This work was supported by the U.S. National Science Foundation under Grant ECCS-1546980.

ABSTRACT A liquid-metal RF shunt switch is presented that combines a dielectric spacer over the RF path with electrolyte-filled capillary troughs to facilitate low-power electrical actuation. The switch demonstrates between 20- and 30-dB isolation in the dc to 5-GHz range, and greater than 10-dB isolation from 5 to 11 GHz. This switch has between 0.2- and 1.2-dB insertion loss from dc to 5 GHz.

INDEX TERMS Gallium alloys, switches, microwave devices.

I. INTRODUCTION

An RF shunt switch creates a path to ground for a signal between two ports. Many shunt-style switches use PIN diodes to create this path to ground, but this typically introduces an undesirable frequency dependence [1]. Wide-bandwidth MEMS switches can eliminate this dependence, but often require high actuation voltages [2]. Liquid metal potentially addresses both of these issues by providing broad frequency performance without the need for high voltages.

Liquid metals for switches have been previously demonstrated using mercury [3], but the toxicity of mercury makes these switches potentially harmful if the packaging is compromised. More recently, non-toxic gallium-based liquid metals, such as eutectic gallium-indium (EGaIn) and gallium-indium-tin (Galinstan), have been used in liquid-metal switches [4]–[7] and in other reconfigurable RF devices [8], including antennas [9] and filters [10], [11].

Non-toxic liquid-metal switches have utilized pressure-driven actuation using syringes or micropumps [4], [7], or high-voltage actuation like electrowetting-on-dielectric [5]. Pressure-driven liquid-metal switches such as [4] have achieved operating ranges from 2 to 100 GHz by using a mechanical pump. The switch in [5] demonstrated 0.3 dB insertion loss across a dc to 40 GHz range, but used a continuously applied 100-V bias for switching.

Recently, electrical actuation of liquid metal has been demonstrated using low-voltage, low-power signals [12], [13]. However, when liquid-metal switches have used these actuation techniques, they suffered from degraded performance due to the lossy electrolyte commonly used for actuation [6].

This paper presents a coplanar waveguide (CPW) liquid-metal shunt switch that combines a low-voltage electrical actuation mechanism, simplified fabrication, and reduced insertion loss relative to previous designs.

II. DESIGN

A. CONCEPT

The switch is composed of two main components: a CPW transmission line and a polyimide channel with a polystyrene cap for the liquid metal [Fig. 1(a)]. The channel is placed perpendicular to the signal line, bridging the gaps between the CPW signal line and ground planes.

A shunt connection to ground is created by positioning a liquid-metal slug over the signal line and bridging the gaps to both coplanar grounds [Fig. 1(b)]. Repositioning the liquid metal to either side removes the connection between signal line and ground [Fig. 1(c)].

B. LIQUID-METAL ACTUATION AND THE USE OF A DIELECTRIC SPACER

Liquid metal is moved with the use of low-power, low-voltage continuous electrowetting (CEW). CEW creates a difference in the interfacial surface tension along a volume of liquid metal immersed in an electrolyte [12], consequently inducing the movement of liquid metal in the direction of positive voltage (Fig. 2). The switch is actuated with an 8-V_{pp} square wave with a 4-V_{dc} offset, operating at 30 Hz and a 50% duty cycle [12]. Actuating the switch with this CEW technique requires less than 16 mW while switching, and once the desired on or off position is reached the actuation signal is manually removed.

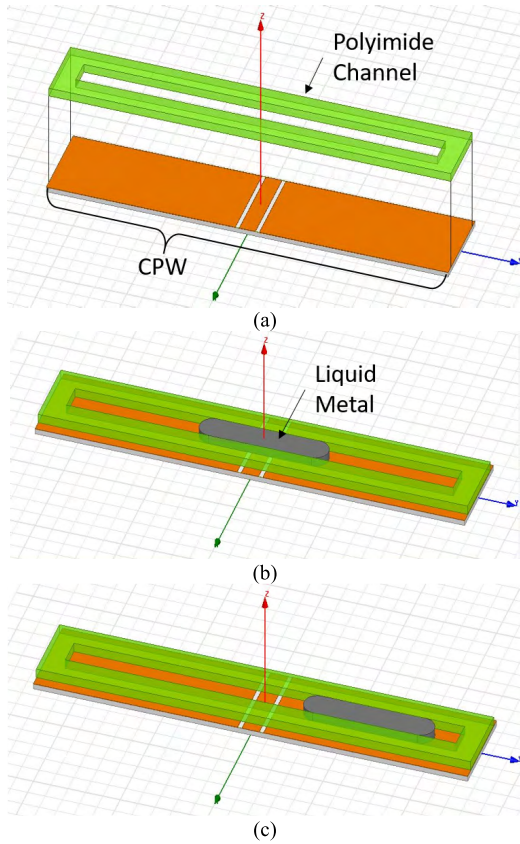


FIGURE 1. Layout of the liquid-metal switch. a) Basic components of the switch. b) Shunt ON state. c) Shunt OFF state. A polystyrene layer (not shown) caps the channels.

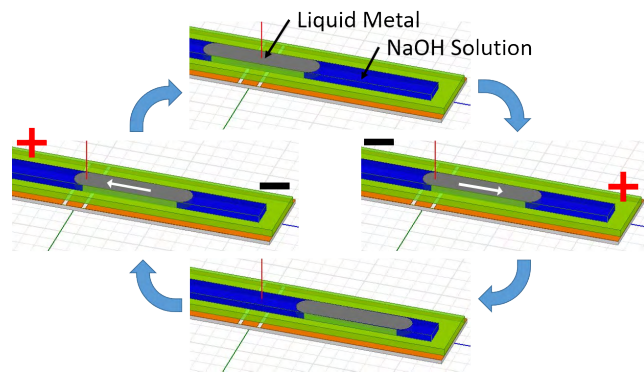


FIGURE 2. Continuous electrowetting is used to move the liquid-metal slug in the direction of the positive probe. Reversing the applied signal returns the slug to the original position.

A continuous electrolyte path between the actuation probes and the liquid metal is necessary for CEW, but water-based electrolyte solutions, such as the 1-M sodium hydroxide (NaOH) solution used here and elsewhere [6], [14], have appreciable RF losses. When the electrolyte occupies the channel above the signal line it absorbs the RF signal, degrading the insertion loss of the switch (Fig. 3). An intuitive solution is to remove the electrolyte between actuations

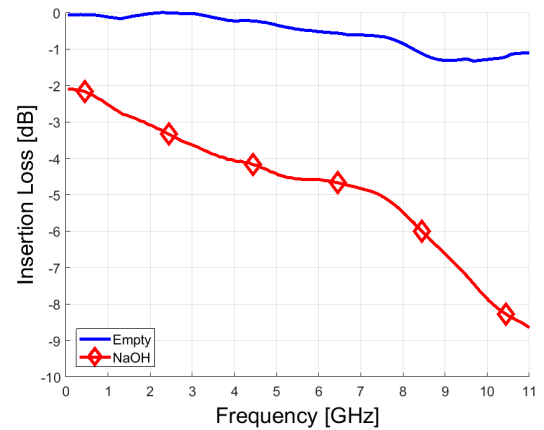


FIGURE 3. Degradation in insertion loss between CPW with an empty channel (blue) and an electrolyte-filled channel (red). Filling the polyimide channel with the NaOH solution used for actuation increases the insertion loss of the CPW by 2 to 8 dB.

and replace the fluid when actuation is needed. However, this time- and power-consuming process requires a separate pumping operation to remove and replace the electrolyte, partially negating the benefits of using CEW.

An alternative technique was introduced in [15], where an air bubble was used as a dielectric spacer to displace the electrolyte. However, the addition of the air bubble blocks the CEW actuation signal, so the device in [15] was pressure-actuated. This paper adapts the air-bubble concept to a CEW-actuated switch by adding narrow capillary troughs above the channel, and is an expansion on the work first reported in [14]. The troughs provide a path for the actuation signal while an air bubble resides between two liquid-metal slugs in the main channel, enabling the use of CEW. To create these troughs, an additional polyimide layer is added above the main channel (Fig. 4). The capillary layer is wider than the main channel, creating the capillary troughs (Fig. 5).

C. CAPILLARY TROUGHS

The capillary troughs contain the electrolyte, but exclude the air bubble and liquid metal, creating an uninterrupted path for the CEW actuation signal through the electrolyte, while keeping the air bubble in place between the liquid-metal slugs. This is achieved through the high surface tension of the liquid metal and the capillary action experienced by the electrolyte.

Liquid metal has a surface tension between 500 and 700 mN/m [16]. Liquids with high surface tension resist an increase in their surface area in the absence of an external force. If the liquid metal were to enter the troughs at the top of the main channel, its surface area would increase (Fig. 5). Thus, the high surface tension of liquid metal prevents it from being moved into the smaller capillary troughs during actuation, and capillary action on the electrolyte draws the liquid into the troughs preferentially over the air bubble. An air bubble introduced into the main channel then can be

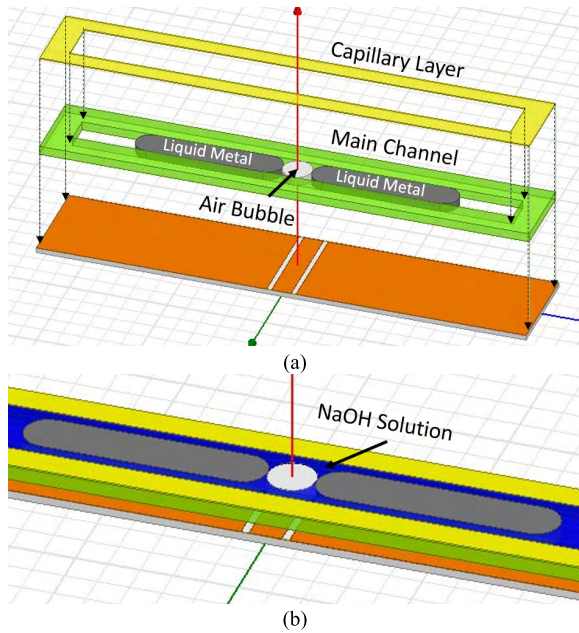


FIGURE 4. Structure of the modified switch with an air bubble positioned between two liquid-metal slugs. (a) Exploded view of the layers of the modified switch. The capillary layer is added above the main channel to maintain the actuation path for continuous electrowetting. The channel is covered with a layer of polystyrene (not shown). (b) The modified switch layout. The NaOH solution (blue) is continuous in the capillary trough across the length of the channel.

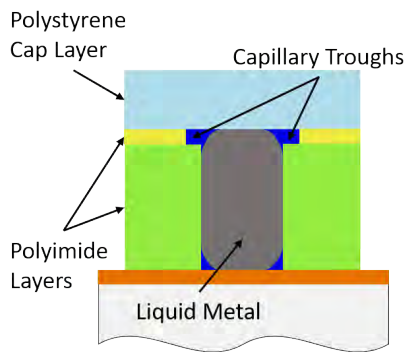


FIGURE 5. The addition of a polyimide layer with a wider channel above the main channel creates capillary troughs above the main channel. The liquid metal does not enter the troughs. The electrolyte solution experiences capillary forces that wick the solution into the narrow capillary troughs preferentially, maintaining the electrolyte path necessary for CEW actuation even if an air bubble is present in the main channel.

used as a dielectric spacer that does not sever the electrical connection between the liquid metal and the actuation probe on opposite sides of the air bubble, but displaces the lossy electrolyte.

D. MATERIAL COMPATIBILITY

Gallium-based liquid metals are reactive with many common metals [17]. For example, liquid metal will stick to a copper surface, making it difficult to move using CEW. To prevent this, tungsten wires [6] and Cr/Ni [5] have been used as switch contacts in previous designs. As chromium and nickel are two major non-iron components in stainless steels, stainless-steel

pads were used as a rapidly prototyped alternative to Cr/Ni switch contacts. The stainless-steel pads allow direct metal-to-metal contact between the liquid metal and CPW ground plane, in contrast to the design in [14] in which the capacitive contact between liquid metal and ground plane hampered low-frequency operation.

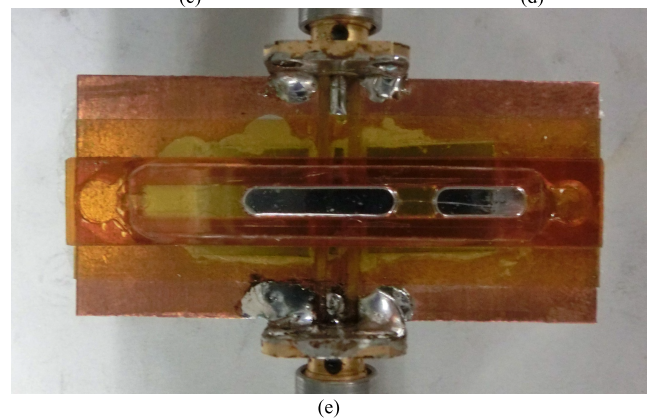
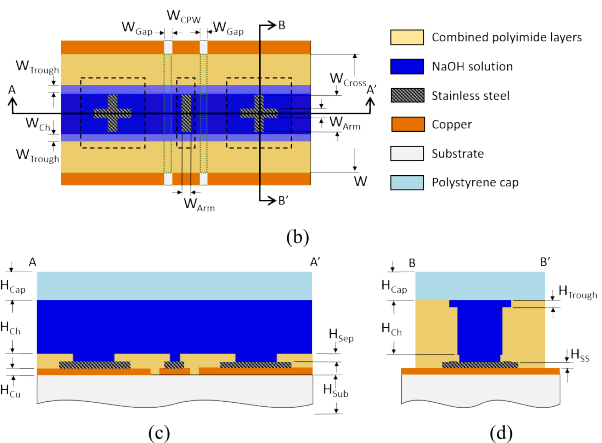
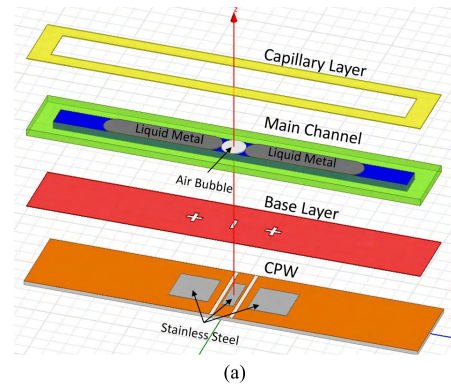


FIGURE 6. (a) Exploded view of the final switch design. (b) Top view of the switch structure without liquid metal or air bubble. (c) Side view of the switch structure. (d) Cross-section of the switch structure. The length of the switch and the polyimide switching structure is 50 mm, the switch width is 10 mm, and the width of the polyimide structure (W) is 8 mm. Additional channel dimensions are shown in Table 1. (e) Photo of the fabricated switch in the shunt ON state.

E. FABRICATION

The switch is fabricated by layering materials over the CPW transmission line (Fig. 6). First, silver epoxy is used to adhere

TABLE 1. Channel dimensions (mm).

$W_{Trough} = 0.75$	$W_{Ch} = 3$	$W_{Cross} = 2$	$W_{Arm} = 0.5$
$W_{CPW} = 2$	$W_{Gap} = 0.9$	$H_{Cap} = 1$	$H_{Trough} = 0.1$
$H_{Ch} = 0.9$	$H_{Cu} = 0.035$	$H_{SS} = 0.051$	$H_{Sep} = 0.1$
$H_{Sub} = 1.27$			

thin stainless-steel pads to the center conductor and ground planes. Then the gaps between the CPW conductors are filled with a layer of polyimide to create a level floor, and a base layer of polyimide tape is placed over the CPW and stainless steel structure. The base layer has a rectangular hole, 2 mm × 0.5 mm, over the center conductor and cross-shaped holes, 2 mm square with arms 0.5 mm wide, above the ground planes [Fig. 6(b)]. The rectangle and irregular cross shapes are variations on the metastable locking notches in [6] and allow the liquid metal to contact the underlying CPW.

Guidelines for the channel design are based on [12], [13]. The channel structure is built atop the base layer by adding 0.1-mm polyimide layers up to the desired height, H_{ch} [Fig. 6(c), (d)]. The channel in the top layer of polyimide is 1.5 mm wider than in the lower layers, thus forming the 0.75-mm-wide capillary troughs running along the length of the main channel on either side. Finally, a polystyrene cap is placed on top to create the ceiling. The finished channel cross-section is 0.9 mm × 3 mm, discounting the capillary troughs, for a height-to-width ratio of 0.3.

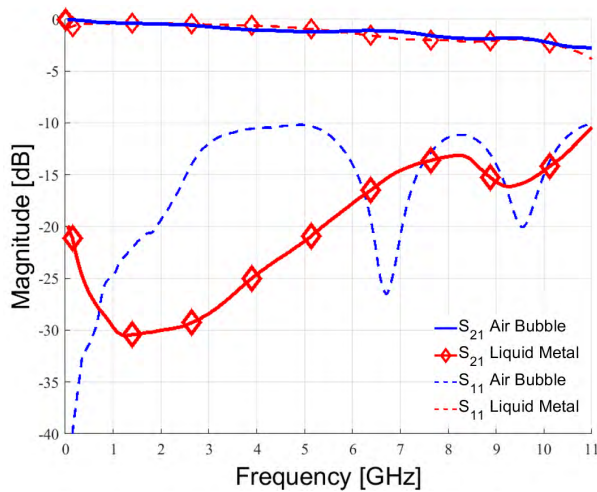


FIGURE 7. Measured S_{21} (solid) and S_{11} (dashed) of the ON/OFF states of the switch. Isolation of the shunt ON state (Liquid Metal red solid line) is greater than 10 dB. Insertion loss of the shunt OFF state (Air Bubble blue solid line) of the switch is less than 3 dB.

III. RESULTS

The final switch design includes two liquid-metal slugs and an air bubble as a switching mechanism. Fig. 7 shows the measurements of the switch in its two states. Measurements were made with an Agilent 8720ES network analyzer. An Agilent 33210A function generator was used for the CEW actuation.

In the shunt ON state, liquid metal is placed over the CPW. The S_{21} measurement, shown in Fig. 7 as the solid red line, represents the isolation between Ports 1 and 2, with the results showing between 20 dB and 30 dB isolation from dc to 5 GHz, and greater than 10 dB isolation up to 11 GHz. The S_{11} measurement, shown in Fig. 7 as the dashed red line, is the return loss of the switch, and is between 0.3 and 5 dB.

In the shunt OFF state, the air bubble is placed over the CPW. In this state, the S_{21} measurement, shown as the solid blue line in Fig. 7, represents the insertion loss of the switch. This is 0.2 to 2 dB (including the loss of the two SMA connectors and the CPW transmission line) from dc to 8 GHz and 2 to 3 dB from 8 to 11 GHz. The return loss in this state, shown as the dashed blue line in Fig. 7, is between 10 and 30 dB from 0.5 to 11 GHz.

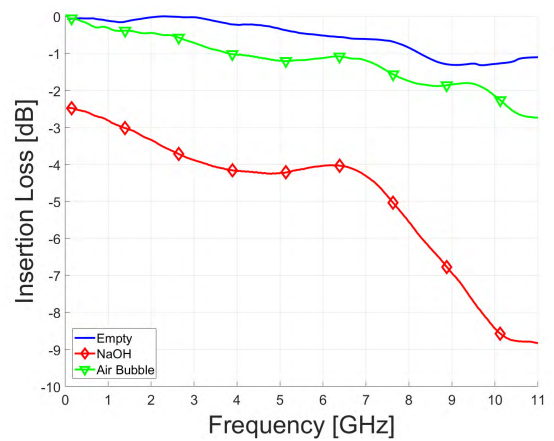


FIGURE 8. Degradation in insertion loss between CPW with an empty channel, an NaOH-filled channel, and a channel with electrolyte displaced by an air bubble.

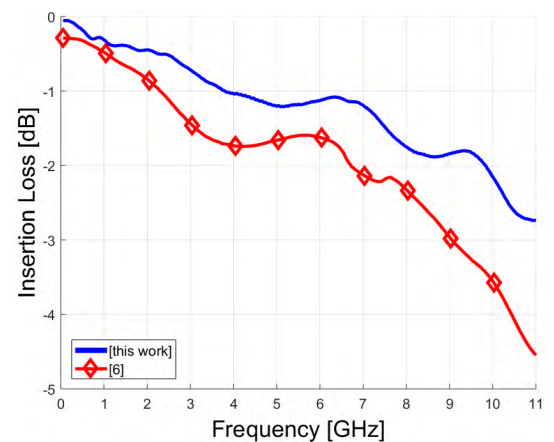


FIGURE 9. The addition of an air bubble improves the insertion loss of this switch by an average of 1.7 dB relative to a similar CPW switch that does not use an air bubble [6].

Fig. 8 compares an empty channel, an NaOH-filled channel, and a channel with an air bubble, demonstrating how using an air bubble improves the insertion loss by reducing the amount of lossy electrolyte near the RF signal path.

Without the air bubble, the insertion loss increases by as much as 7 dB relative to an empty channel with no NaOH. Positioning the bubble over the gaps brings the insertion loss back within 2 dB of the original CPW structure (the empty channel). This combination of electrolyte with an air bubble enables repeatable CEW actuation while reducing exposure to lossy electrolyte.

A similar CPW switch design [6] that did not use an air bubble to displace the electrolyte is compared to this design in Fig. 9. This design improves the insertion loss by an average 1.7 dB across the reported range.

The switching time is related to the speed at which liquid metal moves during CEW actuation. The 8-V_{pp} actuation signal moves the liquid metal at 3 mm/s, comparable to CEW actuation without the presence of an air bubble [12], taking 0.3 s/mm to change between states. The liquid metal needs to move 7.5 mm to position the dielectric spacer, with 2.25-s switching time. Scaling down the size of the switch will decrease this time.

IV. CONCLUSION

A liquid-metal switch was presented that achieves between 10 dB and 30 dB isolation across a dc to 11 GHz operating range. CEW, a low-power electrical actuation technique, was used to switch between states, and a dielectric spacer was introduced to counter the lossy dielectric solution needed for this technique. The use of the dielectric spacer reduces the insertion loss to between 0.2 and 3 dB. The 8-V_{pp} actuation voltage is an order of magnitude less than that of typical PIN diode (~28 V and 100 mA) and MEMS (~30–90 V) switch dc requirements.

REFERENCES

- [1] "Understanding RF/Microwave solid state switches and their applications," Keysight Technol., Santa Clara, CA, USA, Appl. Note 5989-7618EN, 2016.
- [2] G. M. Rebeiz, C. D. Patel, S. K. Han, C. H. Ko, and K. M. J. Ho, "The search for a reliable MEMS switch," *IEEE Microw. Mag.*, vol. 14, no. 1, pp. 57–67, Jan./Feb. 2013.
- [3] P. Sen and C.-J. Kim, "Microscale liquid-metal switches—A review," *IEEE Trans. Ind. Electron.*, vol. 56, no. 4, pp. 1314–1330, Apr. 2009.
- [4] C. H. Chen and D. Peroulis, "Liquid RF MEMS wideband reflective and absorptive switches," *IEEE Trans. Microw. Theory Techn.*, vol. 55, no. 12, pp. 2919–2929, Dec. 2007.
- [5] P. Sen and C. J. Kim, "A liquid–solid direct contact low-loss RF micro switch," *J. Microelectromech. Syst.*, vol. 18, no. 5, pp. 990–997, Oct. 2009.
- [6] G. B. Zhang, R. C. Gough, M. R. Moorefield, A. T. Ohta, and W. A. Shiroma, "An electrically actuated liquid-metal switch with metastable switching states," in *IEEE MTT-S Int. Microw. Symp. Dig.*, San Francisco, CA, USA, May 2016, pp. 1–4.
- [7] N. Vahabisani, S. Khan, and M. Daneshmand, "A K-band reflective waveguide switch using liquid metal," *IEEE Antennas Wireless Propag. Lett.*, vol. 16, pp. 1788–1791, Mar. 2017.
- [8] J. H. Dang, R. C. Gough, A. M. Morishita, A. T. Ohta, and W. A. Shiroma, "Liquid-metal-based reconfigurable components for RF front ends," *IEEE Potentials*, vol. 34, no. 4, pp. 24–30, Jul./Aug. 2015.
- [9] D. Rodrigo, L. Jofre, and B. A. Cetiner, "Circular beam-steering reconfigurable antenna with liquid metal parasitics," *IEEE Trans. Antennas Propag.*, vol. 60, no. 4, pp. 1796–1802, Apr. 2012.
- [10] N. Vahabisani, S. Khan, and M. Daneshmand, "Microfluidically reconfigurable rectangular waveguide filter using liquid metal posts," *IEEE Microw. Wireless Compon. Lett.*, vol. 26, no. 10, pp. 801–803, Oct. 2016.

- [11] J. H. Dang, R. C. Gough, A. M. Morishita, A. T. Ohta, and W. A. Shiroma, "A tunable X-band substrate integrated waveguide cavity filter using reconfigurable liquid-metal perturbing posts," in *IEEE MTT-S Int. Microw. Symp. Dig.*, Phoenix, AZ, USA, May 2015, pp. 1–4.
- [12] R. C. Gough, A. M. Morishita, J. H. Dang, W. Hu, W. A. Shiroma, and A. T. Ohta, "Continuous electrowetting of non-toxic liquid metal for RF applications," *IEEE Access*, vol. 2, pp. 874–882, Aug. 2014.
- [13] R. C. Gough, A. M. Morishita, J. H. Dang, M. R. Moorefield, A. T. Ohta, and W. A. Shiroma, "Rapid electrocapillary deformation of liquid metal with reversible shape retention," *Micro Nano Syst. Lett.*, vol. 3, no. 1, pp. 1–9, Apr. 2015.
- [14] M. R. Moorefield, R. C. Gough, J. H. Dang, A. T. Ohta, and W. A. Shiroma, "A planar liquid-metal shunt switch," in *Proc. IEEE/ACES Int. Conf. Wireless Inf. Technol. Syst. (ICWITS) Appl. Comput. Electromagn. (ACES)*, Honolulu, HI, USA, Mar. 2016, pp. 1–2.
- [15] J. H. Dang, R. C. Gough, A. M. Morishita, A. T. Ohta, and W. A. Shiroma, "Liquid-metal frequency-reconfigurable slot antenna using air-bubble actuation," *Electron. Lett.*, vol. 51, no. 21, pp. 1630–1632, Oct. 2015.
- [16] T. Liu, P. Sen, and C.-J. Kim, "Characterization of nontoxic liquid-metal alloy galinstan for applications in microdevices," *J. Microelectromech. Syst.*, vol. 21, no. 2, pp. 443–450, Apr. 2012.
- [17] R. N. Lyon, *Liquid-Metals Handbook*, 2nd ed. Washington, DC, USA: U.S. Atomic Energy Commission, 1952, ch. 4, pp. 170–171.

MATTHEW R. MOOREFIELD (S'14) received the B.S. degree in electrical engineering from the University of Hawai'i at Mānoa, Honolulu, HI, USA, in 2014, where he is currently pursuing the M.S. degree in electrical engineering.

He has authored 13 publications on his research in switchable and reconfigurable devices using liquid metal, including antennas and RF switches.



RYAN C. GOUGH (S'13–M'16) received the B.S. degree in electrical engineering from Texas Tech University, Lubbock, TX, USA, in 2006, the M.S. degree in electrical engineering from Southern Methodist University, Dallas, TX, USA, in 2010, and the Ph.D. degree in electrical engineering from the University of Hawai'i at Mānoa, Honolulu, HI, USA, in 2016.

He was an RF Engineer with Lockheed Martin Aeronautics Company (LMAC), Fort Worth, TX, USA, from 2006 to 2011, where he was involved in electromagnetic compatibility testing and production-level antenna characterization. In 2008, he was one of the 25 young engineers selected company-wide for participation in the LMAC Engineering Leadership Development Program, designed to identify and develop future engineering leaders. He is currently an RF Engineer with North Star Scientific Corporation, Kapolei, HI, USA.

Dr. Gough was named the 2014 Scholar of the Year by the Honolulu Chapter of the Achievement Rewards for College Scientists Foundation. His paper on dynamic aperture slot antennas received Second Place in the Student Paper Competition of the 2014 IEEE MTT-S International Microwave Symposium.



AARON T. OHTA (S'99–M'09–SM'15) received the B.S. degree from the University of Hawai'i (UH) at Mānoa, Honolulu, HI, USA, in 2003, the M.S. degree from the University of California at Los Angeles, Los Angeles, CA, USA, in 2004, and the Ph.D. degree from the University of California at Berkeley, Berkeley, CA, USA, in 2008, all in electrical engineering.

In 2009, he joined the University of Hawai'i at Mānoa, where he is currently a Professor of electrical engineering. He has authored over 130 publications in the areas of microelectromechanical systems and microfluidics.

Dr. Ohta was a recipient of the 2012 UH Regents' Medal for Excellence in Research and the 2015 UH Regents' Medal for Excellence in Teaching, the ten-campus UH System's most prestigious research and teaching award, respectively.



WAYNE A. SHIROMA (S'85–M'87–SM'08) received the B.S. degree from the University of Hawai'i (UH) at Mānoa, Honolulu, HI, USA, in 1986, the M.Eng. degree from Cornell University, Ithaca, NY, USA, in 1987, and the Ph.D. degree from the University of Colorado at Boulder, Boulder, CO, USA, in 1996, all in electrical engineering.

In 1996, he joined the UH at Mānoa, where he is currently a Professor and the Chair of electrical engineering. He was also a member of the Technical Staff with Hughes Space and Communications, El Segundo, CA, USA. He has authored over 130 publications in the areas of microwave circuits and antennas, nanosatellites, and engineering education.

Dr. Shiroma served three terms on the IEEE Microwave Theory and Techniques Society (MTT-S) Administrative Committee, from 2002 to 2010, and was the General Chair of the 2007 and 2017 IEEE MTT-S International Microwave Symposiums. He was a recipient of the 2003 UH Regents' Medal for Excellence in Teaching, the ten-campus UH System's most prestigious teaching award. Since 2001, IEEE-HKN, the international honor society for IEEE, recognized four of his graduating seniors as the most outstanding electrical engineering students in the U.S.

...